Journal of Nuclear Materials 390–391 (2009) 330–334

Contents lists available at ScienceDirect

Journal of Nuclear Materials

journal homepage: www.elsevier.com/locate/jnucmat

Particle confinement control with resonant magnetic perturbations at TEXTOR

O. Schmitz [a,*], J.W. Coenen [a], H. Frerichs [a], M. Kantor [d], M. Lehnen [a], B. Unterberg [a], S. Brezinsek [a], M. Clever [a], T. Evans [b], K.H. Finken [a], M. Jakubowski [c], A. Kraemer-Flecken [a], V. Phillips [a], D. Reiter [a], U. Samm [a], G.W. Spakman [d], G. Telesca [a], The TEXTOR team

[a] Institut für Energieforschung – Plasmaphysik, Forschungszentrum Jülich, Association EURATOM–FZJ, Trilateral Euregio Cluster, Germany
[b] General Atomics, PO Box 85608, San Diego, CA 92186-5608, USA
[c] Max Planck Institut für Plasmaphysik, IPP–EURATOM Association, Greifswald, Germany
[d] FOM-Institute for Plasma Physics Rijnhuizen, Trilateral Euregio Cluster, Association EURATOM–FOM, P.O. Box 1207, 3430 BE Nieuwegein, The Netherlands

ARTICLE INFO

PACS:
52.25.Fi
52.55.Fa
51.60.+a

ABSTRACT

Two very contrary particle confinement stages were obtained at TEXTOR-DED by application of resonant magnetic perturbations. On the one hand a spontaneous build up of the total number of particles N_{tot} with correlated increase in the particle confinement time τ_p was observed and on the other hand a controlled decrease of N_{tot} and τ_p – the so called stochastic particle pump out is seen. Numerical analysis of the perturbed magnetic field topology shows that both domains can be distinguished by the ratio of short connection length field lines touching a specific resonant flux surface (here the $q = 5/2$ surface) to the complete perturbed layer width. During improved particle confinement, the hyperbolic fixed points (X-points) of the pitch resonant islands are directly connected to the DED target followed by an $\lesssim 40\%$ increase in τ_p. The subsequent increase in the $E \times B$ shear rate $\Omega_{E\times B}$ at the $q = 5/2$ surface and a steepening of $\nabla n_e(r)$ suggests a reduction of the radial particle transport. On the opposite, complete stochastisation of this island chain, i.e. a predominant diffusive field line characteristics, causes a $\lesssim 30\%$ decrease of τ_p with a reduction in $\Omega_{E\times B}$ at the $q = 5/2$ surface and $\nabla n_e(r)$ indicating enhanced effective outward particle transport.

1. Introduction

Perturbation of the confining magnetic field by resonant magnetic perturbations (RMP) is a modern method to control the plasma edge transport. It facilitates particle and energy exhaust in the island and helical divertor concepts for stellarators [1]. In poloidally diverted H-mode plasmas, application of RMP allows for mitigation [2] and complete suppression [3] of harmful edge localized modes. Here, particle pump out has been observed [4] and 2D modeling with *SOLPS*5 [5] as well as 1D analytical modeling [6] suggest an enhanced radial particle transport due to magnetic field line diffusion explaining the decrease in the particle confinement observed. The application of RMP in future fusion devices such as ITER and W7-X requires an understanding of the perturbed magnetic field structure and the correlated modification of transport.

At TEXTOR the dynamic ergodic divertor was designed as a flexible tool investigating various aspects in application of RMP [7]. The poloidal (m) and toroidal (n) base mode numbers of the resonance spectrum can be set to $m/n = 3/1, 6/2, 12/4$. Variation of the base mode spectrum as well as of the plasma equilibrium modifies the perturbed magnetic topology and transport characteristics of the perturbed edge layer induced [8]. Herewith, a fair agreement between plasma structures and the vacuum modeled perturbed field structure was revealed unless tearing modes are driven by the DED field [9]. In this contribution it is demonstrated that by application of the DED induced RMP field an improvement of the particle confinement [10] as well as a controlled deconfinement – the so called stochastic particle pump out – can be achieved and a correlation of both confinement stages to the vacuum modeled magnetic field topology is shown.

2. Experimental observation of improved particle confinement and particle pump out

Application of the DED produced RMP field leads to a characteristic increase and decrease in N_{tot} and the actual change depends on the level of edge stochastisation. To show this, we discuss in this section results from two discharges with similar equilibrium at $q_a = 3.5$ and therefore with comparable coupling of the DED imposed RMP field in $m/n = 6/2$ base mode. Both discharges were positioned in the center of the vessel at $R_0 = 1.75$ m which means that both, the ALT-II belt limiter as well as the DED target surface covering the complete center post area represent the limiting

* Corresponding author.
E-mail address: o.schmitz@fz-juelich.de (O. Schmitz).

0022-3115/$ - see front matter © 2009 Elsevier B.V. All rights reserved.
doi:10.1016/j.jnucmat.2009.01.149

surfaces. The only quantity changed in between the two discharges is the ratio B_r/B_T of the perturbing field B_r to toroidal field B_T due to adaptations of B_T for diagnostic purposes by 10%. Therefore, practically these discharges were identical in the experimentally setup and the only quantity changed for analysis purpose was the DED current I_{DED} in order to obtain both particle confinement stages investigated.

In Fig. 1, the occurrence of a spontaneous density build up at a very moderate level of $I_{DED} = 1.75$ kA is shown. The line averaged, central electron density time trace $n_{e\,l.a.}(t)$ is depicted with left ordinate in green color (please see electronic version of paper for color figures) for the no-DED reference discharge and in blue with perturbation applied. The density increases by 15% at $t = 2.0$ s while $T_e(t)$ measured at the plasma center (right ordinate, with black for perturbed and magenta for unperturbed discharge), stays constant. The obvious increase in the energy confinement follows the positive density scaling of τ_E at TEXTOR [10]. Fig. 2 shows the radial profiles of $n_e(z)$ and $T_e(z)$ for the complete plasma column and the gradients $\nabla n_e(z)$ and $\nabla T_e(z)$ from Thomson scattering with blue color for the unperturbed case and red with perturbation applied. A clear steepening of the density gradients in the plasma edge region ($0.18\text{ m} < z < 0.3\text{ m}$) is apparent while $\nabla n_e(z)$ and $\nabla T_e(z)$ remain unchanged further inside. The profile flattening on the very boundary can be explained by the laminar zone and localized magnetic flux tubes [8]. As the Thomson scattering system is not on the magnetic axis of this plasma equilibrium [11], the inner boundary of the gradient steepening region was mapped to the plasma equilibrium. The values in normalized poloidal flux Ψ_N are displayed in Fig. 2 which shows that steepening of the gradient for this particular discharge was limited to a region of $\Psi_N > 0.92$.

Raising the DED current further causes vanishing of the density increase and leads instead to decreasing N_{tot} in even correlation to I_{DED} as shown in Fig. 3. The color and ordinate conventions are as

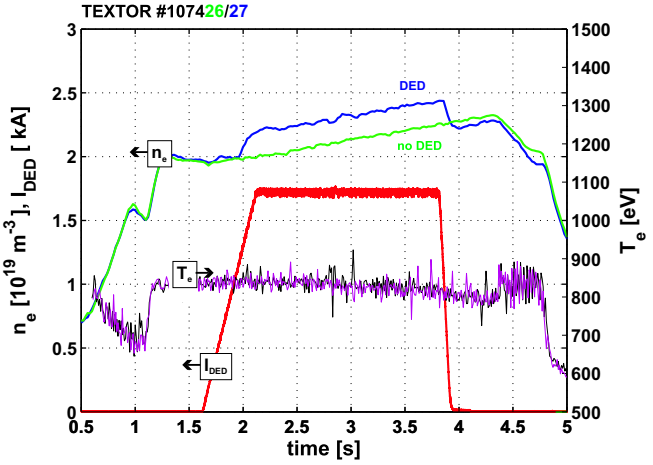

Fig. 1. Electron density $n_e(t)$ (left ordinate) build up in correlation to the electron temperature $T_e(t)$ (right ordinate) and to the DED current $I_{DED}(t)$ (left ordinate). Here $n_e(t)$ with out DED (#107426) is compared to a case with a density increase due to DED application (#107427).

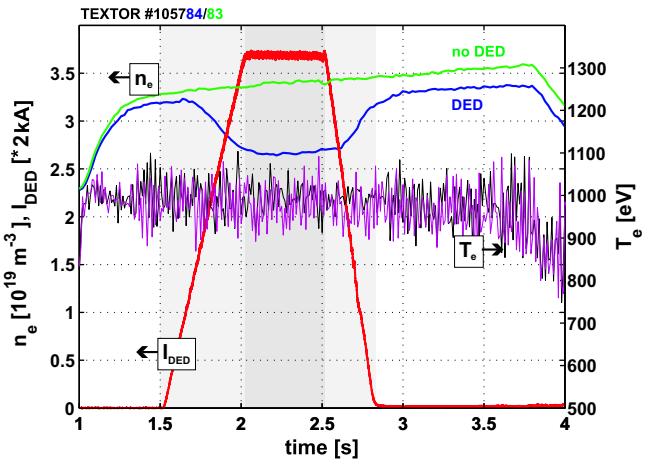

Fig. 3. Electron density $n_e(t)$ (left ordinate) reduction in correlation to the electron temperature $T_e(t)$ (right ordinate) and to the DED current $I_{DED}(t)$ (left ordinate). Here, $n_e(t)$ with out DED (#105783) is compared to a case with a density decrease due to DED application (#105784).

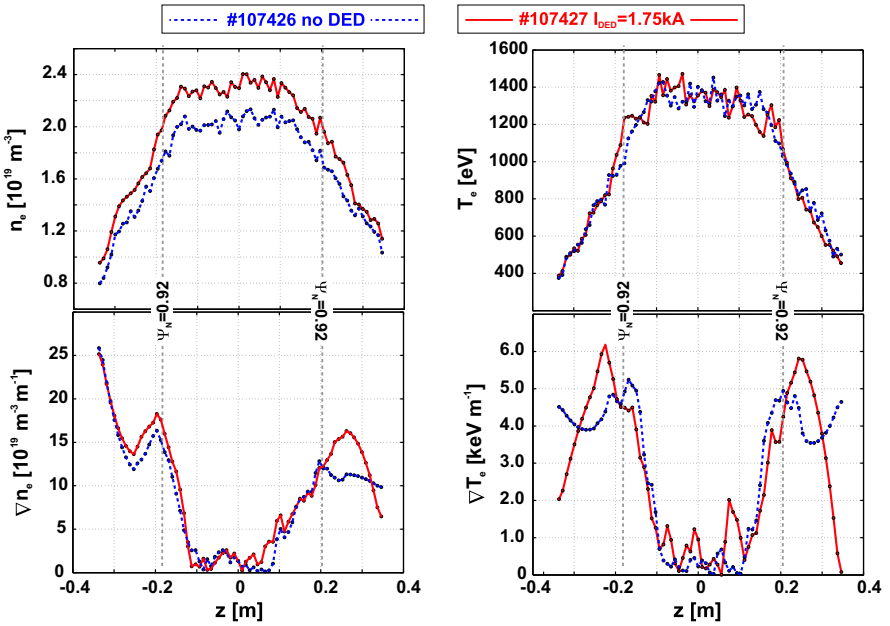

Fig. 2. Electron density $n_e(r)$ and temperature $T_e(r)$ (upper row) and their gradients $\nabla n_e(r)$ and $\nabla T_e(r)$ (lower row) from Thomson scattering. Both, $n_e(r)$ and $T_e(r)$ profiles steepen in $0.92 < \Psi_N$ during the density increase indicating a reduced radial transport in this region.

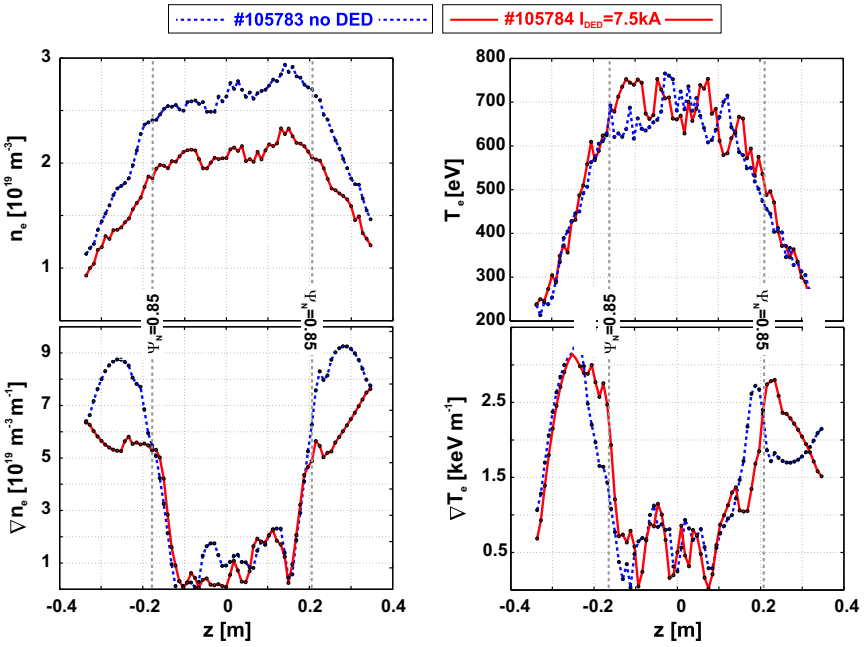

Fig. 4. Electron density $n_e(r)$ and temperature $T_e(r)$ (upper row) and their gradients $\nabla n_e(r)$ and $\nabla T_e(r)$ (lower row) from Thomson scattering. Here, $n_e(r)$ flattens in $0.85 < \Psi_N$ during the density reduction indicating an increased outward particle transport while a maintained or even slightly increasing $T_e(r)$ gradient show marginal change of radial conductive energy transport.

before. In contrast $T_e(t)$ stays unaffected showing a convective loss of confined energy. Fig. 4 shows in the same layout as before $n_e(z)$ and $T_e(z)$ profiles and gradients $\nabla n_e(z)$ and $\nabla T_e(z)$. Here a flattening of $\nabla n_e(z)$ by 30% in maximum and localized in $\Psi_N > 0.85$ is apparent. The extension of this region with modified gradients increases from $\Psi_N = 0.92$ to $\Psi_N = 0.85$ between these two confinement stages. The changes in gradients for the particle pump out compare well to a diffusion dominated picture as described e.g. in [5,6], where an increased particle transport is explained by an increase of the effective outward particle diffusivity $D_{\perp\,eff}$. In contrast, the increase in gradients connected to the density increase points to an improvement in confinement and reduction of transport as indicated in measurements of the $E \times B$ shear rate $\Omega_{E\times B}$. This is discussed in the last section of this paper. Before we describe the particle balance applied in order to quantify the changes in confinement in measures of particle confinement times τ_p and τ_p^*.

3. Particle balance

The time dependent global particle balance in a single reservoir model reads:

$$\frac{dN_{tot}}{dt} = -\frac{N_{tot}}{\tau_p} + f_{rec}\Phi_{rec} + \Phi_{ext} = \Phi_{ext} - \Phi_{pump}, \qquad (1)$$

with the total number of electrons N_{tot}, the recycling flux Φ_{rec} with the fueling rate f_{rec} and the external flux $\Phi_{ext} = f_{NBI}\Phi_{NBI} + f_{gas}\Phi_{gas}$ with the fueling rate f_{NBI} for the neutral beam influx and f_{gas} for the gas influx. These fueling rates are difficult to measure and they are matter of changes in the plasma edge parameters. However, for sake of simplicity we use $f_{rec} = 0.7$, $f_{NBI} = 1.0$ and $f_{gas} = 0.1$ as values used in the particle balance studies for radiative improved mode (RI-mode) experiments at TEXTOR [12].

The most challenging ingredient to determine τ_p is the recycling flux Φ_{rec} on the wall elements. To extract this quantitatively from experiment a tangentially viewing CCD camera (camera 4 described in [11]) was used. It observes about 1/3 of the toroidal circumference of the different wall areas in TEXTOR, including the carbon DED target on the inner wall, the two poloidal limiters and one complete ALT-II blade. Therefore, these lines of sight allow to cover the three-dimensional features of the perturbed edge layer under DED application [8]. It is important to note that for the given discharge setup with plasma centered at $R_0 = 1.75$ m in the vessel, none of the limiting surface protrudes into the perturbed edge layer but the are intersected by the perturbed field lines diverging radially outward due to the DED perturbation at the high field side (HFS). There is no rapid transition between the limiter setup and the perturbed boundary discharge but the stochastic layer establishes linearly with increasing DED current [8,9].

An extended description of a particle balance similar to the one applied here and of the underlying assumptions can be found in [13] and the basic atomic and molecular physics is described in [14]. The CCD camera was calibrated against the calibrated flux Φ_{gas} from a gas inlet during a density ramp. This translates the measured CCD intensity $I_{CCD}(t)$ in counts s^{-1} into an absolute recycling particle influx $\Phi_{rec} = \Phi_A + \Phi_M$ as sum of the molecular flux Φ_M and of the atomic flux Φ_A. The conversion factors S/XB and D/XB (see [14]) need to be reflected in this calibration which gives already a direct functional of $I_{CCD}(\Phi_{gas})(t) = c_{cal} \times \Phi_{gas}(t)$. Since the analysis presented in [13], the carbon DED target – covering about 1/4 of the poloidal circumference of TEXTOR inner wall – was implemented. As the discharges discussed here were positioned at a major radius of $R_0 = 1.75$ m both, the ALT-II limiter and the DED target represent major limiting surfaces for the plasma. Therefore, we use in particular for the ionization rate ratios between the different wall elements the ALT-II values for the recycling fluxes on the DED target. In [13], $S/XB_{ALT} = 22$ on ALT-II limiter, $S/XB_{gas} = 20$ on gas feed and $S/XB_{ALT} = 17$ on ICRH limiters (here also poloidal limiters) and the halo emission in between the limiting wall elements was used. As we calibrated I_{CCD} against the gas inlet we take these different S/XB values into account as normalized factors relative to the value for the gas inlet. We also assume negligible density dependence of S/XB for a typical edge plasma T_e range of 20–100 eV [13]. The calibration factor c_{cal} eventually obtained is therefore used as a constant value during analysis and adapted by a ratio of $\Phi_A/\Phi_M \sim 2/3$ for the composition of the gas cloud during calibration [14].

The particle influx injected by the neutral beams Φ_{beam} was calculated from the beam acceleration voltage and the species injected [15] introducing an aperture factor for the opening of the beam duct for power control. The particle influx Φ_{gas} from the three TEXTOR gas inlets was calculated from the pressure drop in each reservoir. This analysis shows that particle inventory is build up by gas feed during the plasma build up ($t \lesssim 1.0$ s) and eventually maintained by a dominant $\Phi_{rec} \simeq 10^{22}$ s^{-1} and the beam injected particles of $\Phi_{beam} \simeq 10^{20}$ s^{-1}. The gas injected building up the plasma density is pumped away to a large fraction (~ 98–99%) as we find $\Phi_{pump} \sim \Phi_{gas}$ during $t \lesssim 1.0$ s. This was reflected in a low fueling efficiency coefficient $f_{gas} = 0.1$ for Φ_{gas}.

Based on this balance, we calculate $\tau_p = N_{tot}/[(-dN_{tot}/dt) + f_{rec}\Phi_{rec} + f_{ext}\Phi_{ext}]$ as particle confinement time and $\tau_p^* = N_{tot}/[(-dN_{tot}/dt) + \Phi_{ext}]$ as effective particle confinement time. Both quantities together allow to characterize the particle confinement and determining the recycling coefficient $R = 1 - (\tau_p/\tau_p^*)$. It is important to note that changes in τ_p are not inevitably related to changes in the radial transport. A model describing this for circular plasmas with a perturbed boundary was introduced in [16]. Here, the stochastic boundary is described as a shell with the inner radius b and the unperturbed minor radius a as outer boundary. This yields to $\tau_p = (n_0 b)/(4 n_e D_\perp) \cdot (a - r)$ for $b \leqslant r \leqslant a$. This 1D description shows that in particular a shrinking effective minor radius b as inner boundary of the perturbed edge, will lead to a decrease in τ_p due to a geometrical effect by introducing a stochastic edge layer.

4. Correlation of particle confinement and magnetic topology

In this section the manipulation of N_{tot} by the RMP applied is analyzed in terms of τ_p and τ_p^* as generic quantities describing particle confinement and their dependency on the effective minor radius b of the stochastic layer is resolved. In dedicated experiments plasma position and q_a were adapted such that stochastisation of one rational flux surface, here i.e. the $q = 5/2$ surface, became dominant. For discharges aiming at an increase in N_{tot}, the local perturbation amplitude $B^r_{5,2}$ was decreased in increasing q_a, i.e. moving the $q = 5/2$ surface away from the perturbation source. The rational for this experiment was the observation described in [10], that the improved confinement occurs stepwise with connecting the X-points of pitch resonant magnetic island chains to the DED target, without destroying the complete island chain. This yields the hypothesis that the confinement stage depends on the level of stochastisation of the innermost perturbed island chain.

In order to deduce the effective minor radius in the perturbed edge layer, we employ numerical modeling of the magnetic topology in the vacuum approximation, i.e. superimposing the RMP field on an axisymmetric equilibrium without any plasma feedback. A heterogenous poloidal structure of different field line connection lengths L_c and a direct correlation to localized transport changes was revealed [8]. For the following analysis we reduce this 3*D* description to averaged radial profiles $L_c(\Psi_N)$, with Ψ_N as normalized poloidal flux and deduce from this the extension of a *laminar zone* and an *stochastic layer* following [17]. The 3*D* traced field lines are analyzed at one toroidal position and the connection length to the target is averaged along the poloidal angle. Subsequently the $L_c(\Psi_N)$ profile is compared to the Kolmogorov length L_K. Herewith, the laminar zone as extension of the scrape off layer with predominant direct parallel transport to the target is distinguished from the stochastic zone. Here, the field line connection length is longer than L_K as typical decorrelation length along field lines and enhanced diffusive transport characteristics shall prevail. Therefore, field lines with $L_c < L_K$ are referred to as laminar zone, field lines with $L_c > L_K$ belong to the stochastic zone.

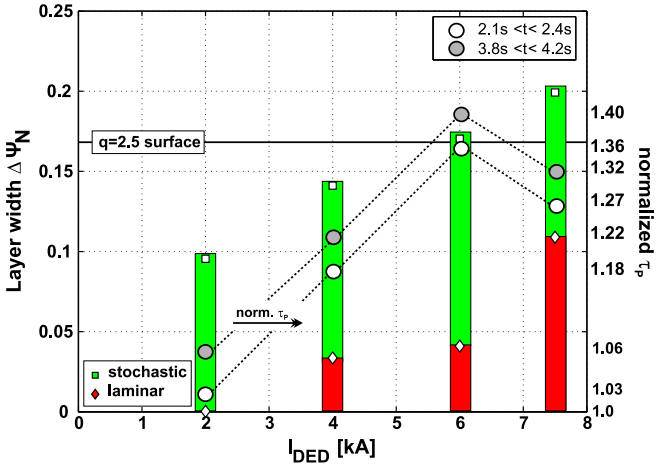

Fig. 5. Increase of the particle confinement time τ_p with I_{DED} and the correspondent evolution of the laminar and stochastic layer width $\Delta\Psi_N$ for the IPC topology.

Fig. 5 shows the results of this analysis of the 3D perturbed edge layer in comparison to τ_p for discharges with density build up on different levels of I_{DED}. The left ordinate shows the width of laminar and stochastic layer as $\Delta\Psi_{N\,lam} = 1 - \Psi_{N\,lam}$ and $\Delta\Psi_{N\,stoch} = 1 - \Psi_{N\,stoch}$. The width of both layers are depicted as bars and the length of the complete bar shows the complete extension of the perturbed edge, i.e. the reduction of the effective minor radius b discussed earlier. The red bars with ♢ markers as boundary depict the laminar layer width while green bars with □ markers as boundary depict the stochastic layer width. In addition the position of the $q = 5/2$ flux surface is indicated as horizontal solid line. The right ordinate shows the change of τ_p normalized to the $I_{DED} = 0$ kA reference discharge. For $I_{DED} = 2.0$ kA the increase is marginal as in comparison to the topology the extension of the perturbed layer is small and the $q = 5/2$ surface is not affected here. Extending the perturbed layer width to this q surface for $I_{DED} = 4.0$ kA and most pronounced for $I_{DED} = 6.0$ kA, τ_p increases showing that the observed increase in N_{tot} is caused by an improvement of the particle confinement. At $I_{DED} = 7.5$ kA, the stochastic layer completely extends to the $\Psi_N(q = 5/2)$ surface and in particular the laminar zone jumps inward. This leads to a reduction of the confinement level reached and represents the transition point towards the particle pump out. The correspondent scan for the particle pump out scenario is shown in Fig. 6 in same layout. The $q = 5/2$ surface was

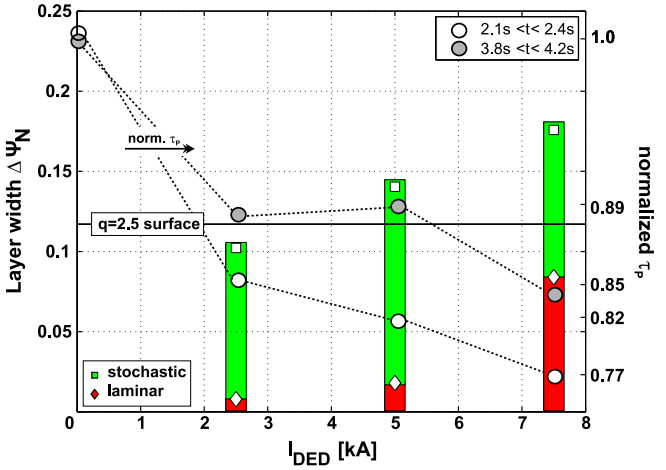

Fig. 6. Decrease of the particle confinement time τ_p with I_{DED} and the correspondent evolution of the laminar and stochastic layer width $\Delta\Psi_N$ for the PO topology.

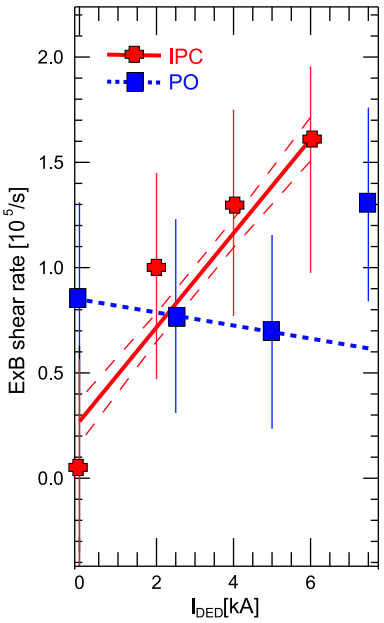

Fig. 7. $E \times B$ shear rate $\Omega_{E\times B}$ at the $q = 5/2$ surface for PO and IPC scenarios as a function of I_{DED}. The increase of $\Omega_{E\times B}$ with I_{DED} at this flux surface potentially reduces the outward transport while a decrease of the $E\times B$ shear rate is capable decreasing the outward transport below the original L-mode transport level.

moved closer to the perturbation source and for same DED currents a reduction of τ_p with increasing DED current was detected. The $q = 5/2$ surface is nearly reached already with $I_{DED} = 2.5$ kA by a large contribution of stochastic field lines. Extending the stochastic layer width over this flux surface leads to a further reduction of τ_p and eventually reaching further in with the laminar zone, as seen for $I_{DED} = 7.5$ kA, leads to a maximum reduction of about $\Delta\tau_p \sim 22\%$. This shows that stochastic field lines with high field line diffusion cause a decrease in particle confinement. Therefore in this case enhanced diffusive radial transport is a possible candidate while a sudden extension of the laminar zone shall be able to reduce the particle confinement due to direct parallel particle losses.

5. Comparison to $E \times B$ shear rate and conclusions

The analysis of τ_p during dedicated changes of the magnetic topology shows that the increase in N_{tot} is caused by an improvement of net particle confinement quantified by τ_p while the stochastic particle pump out shows a degradation of the particle confinement. However, the effective radius b is reduced for both confinement stages showing that the effect observed is not only a geometrical effect. Concerning the plasma source distribution, the analysis of the ionization length λ_{io} shows that it does not experience a strong change but stays roughly constant at $\lambda_{io} \sim 3.5$ cm for comparable density of $n_e = 3.0 \times 10^{19}$ m^{-3}. This means that the manipulation of the dominant plasma source, i.e. the recycling flux Φ_{rec}, is marginal and therefore not an explanation of the particle confinement changes observed. Therefore, the actual change in particle confinement must be linked in a more complex way to the underlying transport. Experimental evidence for transport changes stems from measurements of the radial electric field by means of a hydrogen charge exchange diagnostic beam [18]. Here, a correlated change of the $E \times B$ shear rate $\Omega_{E\times B}$ at the $q = 5/2$ surface was observed as shown in Fig. 7. The discharge series exhibiting an increase in τ_p show an increase in $\Omega_{E\times B}$ at $q = 5/2$ from $\Omega_{E\times B} = 0.2 \times 10^{15}$ s^{-1} to $\Omega_{E\times B} = 1.5 \times 10^{15}$ s^{-1} with increasing DED current. This is in line with $\nabla n_e(r)$ steepening discussed in the beginning and suggests a reduction of radial transport due to enhanced shear and is in agreement with findings on reduced turbulent transport from an analysis in DED $m/n = 3/1$ base mode operation as reported in [19]. For the particle pump out a reduction from $\Omega_{E\times B} = 0.9 \times 10^{15}$ s^{-1} to $\Omega_{E\times B} = 0.6 \times 10^{15}$ s^{-1} is observed and a final increase up to $\Omega_{E\times B} = 1.3 \times 10^{15}$ s^{-1} at the point where the laminar zone as SOL penetrates inward.

This analysis provides substantial evidence that the resulting particle confinement during application of the DED is determined by the fraction of the deeply penetrating field lines to the complete perturbed layer width and the ratio of stochastic field lines. Well dosed perturbation of the plasma edge with a dominant stochastic zone allows for dedicated control of particle confinement while strong perturbation with a deeply penetrating laminar zone strongly degrades the particle confinement. An application of these findings to limiter H-mode plasmas at TEXTOR is discussed in [20]. Here the H-mode pedestal established is degraded in a controlled way with a stochastic layer while it is destroyed as soon as the laminar zone extends the pedestal width. A key question which still remains open is the eventual access of such a dedicated confinement control, i.e. the transition from an improvement in particle confinement to a degradation, the particle pump out. Both effects were observed also at Tore Supra, but here strong changes in the plasma position were mandatory to go from the density increase to a particle pump out phenomenon [22]. The observations presented here from TEXTOR-DED, were obtained purely by adaptation of the local perturbation amplitude on the dominant resonant surface which is the q = 5/2 surface for the setup investigated. The analysis shows that the manipulation of the radial electric field and of the electron density profiles $n_e(r)$ of the compare for the pump out case well to concepts in which enhanced radial ion outflow is caused by manipulation of the radial electric field and poloidal velocity [6] due to open perturbed field lines [21]. However, the contrary reaction observed, i.e. increase in particle confinement and interpretation in terms of transport remains an open challenge for theory.

References

[1] Y. Feng et al., Nucl. Fus. 48 (2008) 024012.
[2] Y. Liang et al., Phys. Rev. Lett. 98 (2007) 265004.
[3] T.E. Evans et al., Nat. Phys. 2 (2006) 419.
[4] E.A. Unterberg et al., J. Nucl. Mater. 390–391 (2009) 486.
[5] S. Mordijck et al., J. Nucl. Mater. 390–391 (2009) 299.
[6] M. Tokar et al., Phys. Plasma 15 (2008) 072515.
[7] K.H. Finken et al., Nucl. Fus. 39 (1999) 637.
[8] O. Schmitz et al., Nucl. Fus. 48 (2008) 024009.
[9] M.W. Jakubowski, O. Schmitz, et al., Phys. Rev. Lett. 96 (2006) 035004.
[10] K.H. Finken et al., Phys. Rev. Lett. 98 (2007) 065001.
[11] O. Schmitz et al., AIP Conf. Proc. 993 (2007) 135.
[12] B. Unterberg et al., Fus. Sci. Technol. 47 (2005) 189.
[13] D.S. Gray et al., Nucl. Fus. 38 (1998) L09.
[14] S. Brezinsek et al., Plasma Phys. Control. Fus. 47 (2005) 615.
[15] R. Uhlemann et al., Fus. Technol. 35 (1998) 42.
[16] Engelhardt, W. Feneberg, et al., J. Nucl. Mater. 76 (1978) 518.
[17] F. Nguyen et al., Nucl. Fus. 37 (1995) 743.
[18] J.W. Coenen et al., in: Europhysics Conference Abstracts, EPS 2008.
[19] A. Kraemer-Flecken et al., Nucl. Fus. 46 (2006) S730.
[20] B. Unterberg et al., J. Nucl. Mater. 390–391 (2009) 351.
[21] B. Unterberg et al., J. Nucl. Mater. 363–365 (2007) 698.
[22] T. Evans, in: Chaos, Complexity and Transport: Theory and Applications, World Scientific Press, Singapore, 2008.